Progress In Electromagnetics Research M, Vol. 127, 113-120, 2024 PIER M

(Received 18 February 2024, Accepted 31 May 2024, Scheduled 16 June 2024)

Four Port MIMO Antenna on Quarter Mode Substrate Integrated Waveguide for Ku Band Applications

Rakhi Kumari* and Shweta Srivastava

Department of Electronics and Communication Engineering, JIIT, Noida, Uttar Pradesh, India

ABSTRACT: In this paper, a miniaturized 4-port (4×4) multiple-input multiple-output (MIMO) antenna is presented in the Ku band with operating frequency range of 16.9 GHz to 17.9 GHz. The presented antenna incorporates Substrate Integrated Waveguide (SIW) Technology with each element of MIMO in Quarter Mode Substrate Integrated Waveguide (QMSIW). The radiating features of the antenna are incorporated by inserting periodic slots in the patches as well as defective ground plane (DGS) technology in lower ground. For achieving good impedance matching and isolation, DGS and SIW technologies are incorporated in the design. An isolation greater than 30 dB is achieved in the complete operating range (16.9 GHz–17.9 GHz). The MIMO antenna is realized physically in Rogers 5880 with dimensions of $36 \times 36\,\text{mm}^2$. The MIMO antenna properties like Envelope Correlation Coefficient (ECC), Channel Capacity Loss (CCL), Total Effective Reflection Coefficient (TARC), Mean Effective Gain (MEG), and Diversity Gain (DG) are analysed to validate good agreement with the standard values.

1. INTRODUCTION

In present day scenario, the trans-receiving channels of wireless communication are highly occupied, and the co-channel interference is very much prominent. Therefore, this area is of keen interest among present day researchers to design an antenna system which will be less susceptible to co-channel interference [5, 7] as well as fading and have high spectral density [1–8]. Also this era is the age of miniaturization, where things are getting more compact day by day. Antennas are getting miniaturized, and MIMO antenna is increasing its impact on market. MIMO antenna increases the channel capacity which in turn increases the data rate, which are two most important parameters of wireless communication [15]. Therefore, MIMO antenna is also a reliable alternative for reducing the co-channel interference. From past few decades when SIW came into existence and when it is further condensed in Half-Mode Substrate Integrated Waveguides (HMSIW) and Quarter-Mode QMSIW, MIMO antenna can be combined with the properties of SIWs and shows very good radiation results [9–11].

The MIMO antenna performance is calculated based on envelope correlation coefficient (ECC), diversity gain (DG), total active reflection coefficient (TARC), channel capacity loss (CCL), and mean effective gain (MEG) [19, 20]. Isolation among the elements of MIMO antenna comes to be approximately below 20 dB as shown in Fig. 5 just by changing the spacing between the elements of quarter mode SIW, inserting vias at left out corner of the quarter mode SIW, and making changes in the ground plane as shown in Fig. 4. The MIMO antenna that has been designed operates in the range of 16.9 GHz and 17.9 GHz as shown in Fig. 6.

The novelty attained by the MIMO antenna is listed as

1. The antenna is designed in a compact size of 36 mm × 36 mm, without compromise on frequency of operation and gain.
2. The antenna with the use of SIW was able to achieve isolation up to 35 dB in such a compact size.
3. In this paper, maximum MIMO parameters are discussed and all are in good agreement with the standard value.

MIMO Parameters	Standard Value	Proposed antenna value
ECC	below 0.5	Below 0.004
DG	10 in ratio	$\approx$ 10 in ratio
TARC	$< 0\,\text{dB}$	$< -5\,\text{dB}$
CCL	less than 0.4 bits/sec/Hz	less than 0.2 bits/sec/Hz
MEG	-3 dB to -12 dB	-3 dB to -4 dB

2. DESIGN PROCESS

The structure shown in Fig. 1 shows the design process of the proposed Quarter Mode Substrate Integrated leaky wave antenna with its design basic as well as sub stage. The antenna is modelled with the help of High Frequency Structure Simulator (HFSS). The first stage of design involves calculating the design parameters of Substrate Integrated Waveguide (SIW) and simultaneously calculating the dominant mode resonant frequency using Equation (1) [12].

$$f_{110}(FM) = \frac{c}{2\sqrt{\varepsilon_{reff}}}\sqrt{\left(\frac{1}{W_{eff}}\right)^2 + \left(\frac{1}{l_{eff}}\right)^2} \tag{1}$$

* Corresponding author: Rakhi Kumari (rakhi.kumari@abes.ac.in).

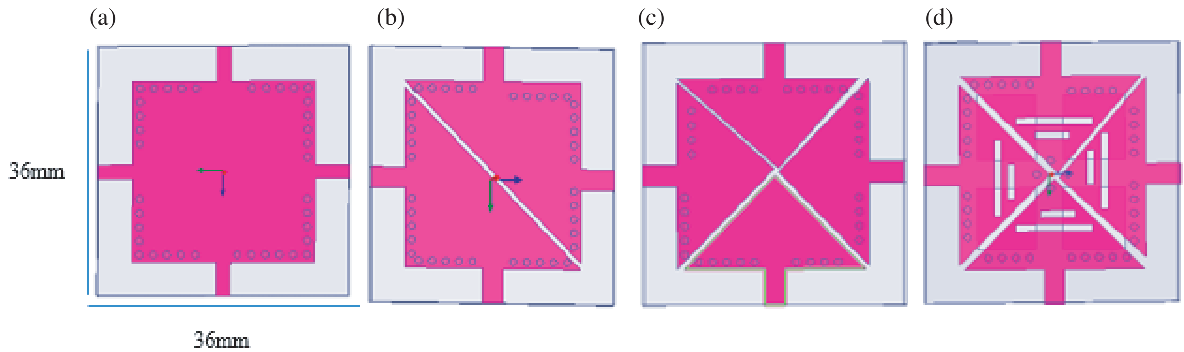

FIGURE 1. Design flow of 4 port MIMO antenna from 4 port FMSIW. (a) Full mode SIW. (b) Half Mode SIW. (c) Quarter Mode SIW. (d) MIMO antenna on Quarter mode SIW.

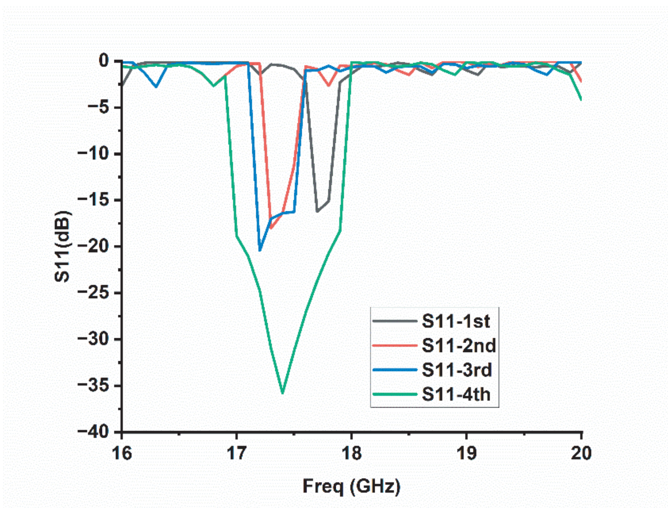

FIGURE 2. Comparison of S_{11} of 4 stages of development of MIMO antenna.

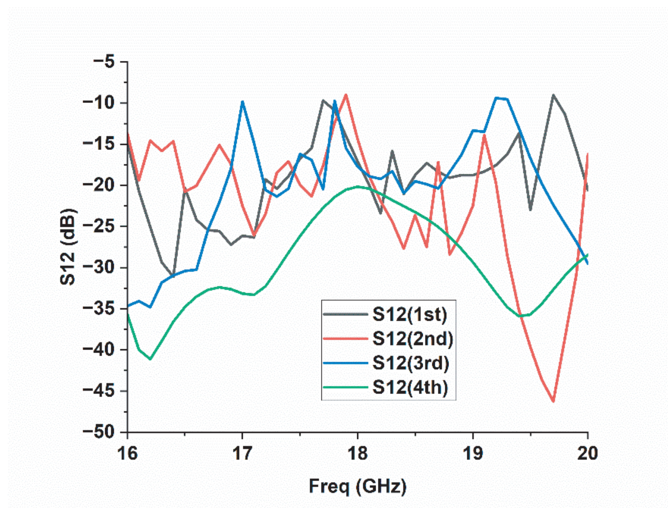

FIGURE 3. Comparison of S_{12} of 4 stages of development of MIMO antenna.

where l_{eff} or $W_{eff} = W$ or $L - \frac{1.08d^2}{p}$, $W_{eff} = W$ and l_{eff} are the effective width and length of the full cavity SIW; d is the diameter of the vias; and p is the space between two adjacent vias.

The quarter mode SIW based MIMO antenna is obtained from full mode SIW as shown in Fig. 1 by bisecting it along its magnetic walls and then using its quarter mode for the design of leaky wave antenna [13, 14]. The dimensions of full mode SIW along with dimension of proposed MIMO antenna are as below:

The S-parameters of different stages of MIMO antenna development are shown in Fig. 2 and Fig. 3. In Fig. 2, S_{11} of all stages of development is shown, and in Fig. 3, S_{12} of all stages of development is shown which clearly interprets that S_{11} which is a reflection coefficient of MIMO antenna gets drastically improved in the 4th stage which is proposed MIMO as compared to its previous stage. Similarly, isolation also gets improved in the 4th stage as shown in Fig. 3.

The QMSIW is constructed with the common ground plane. In each quarter mode, slots are constructed in periodic manner as shown in Fig. 4 so that it starts working as a leaky wave antenna. Since there are four quarter modes created from one full mode SIW, four antennas are created by a common ground plane which make them operate as a MIMO antenna [13, 14]. The 4 antennas operate at approximately same frequency between 16.9 GHz and 17.9 GHz since dimensions of the antennas are also same. For the reduction of inter elemental mutual coupling, the spacing between antenna elements is increased from its previous one as achieved in quarter mode as shown in Fig. 1. As we know, the SIW is the planar replica of dielectric filled rectangular waveguide, and microstrip feed line is incorporated in this to achieve the impedance matching. For further improving the impedance matching, the optimization of feeding location is also done.

The isolation obtained in MIMO antenna is below 30 dB between elements as shown in Fig. 5, and the reflection coefficient which is achieved is below 15 dB in each case as shown in Fig. 6.

3. MIMO ANTENNA

Fig. 4 shows the front and back views of proposed QMSIW leaky wave antenna. The dimensions of antenna are shown in Table 1 and symbolized in Figs. 1 and 4.

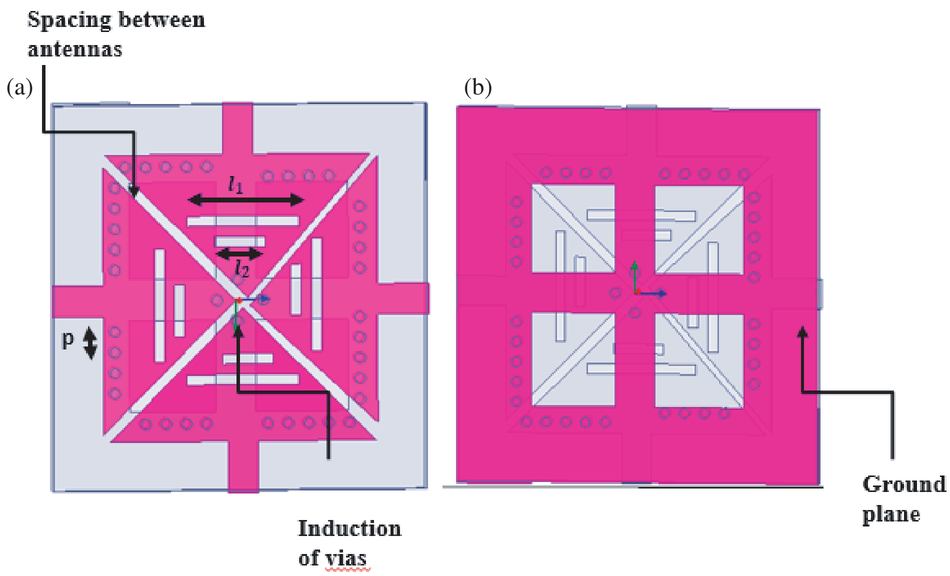

FIGURE 4. MIMO antenna. (a) Top view. (b) Bottom view.

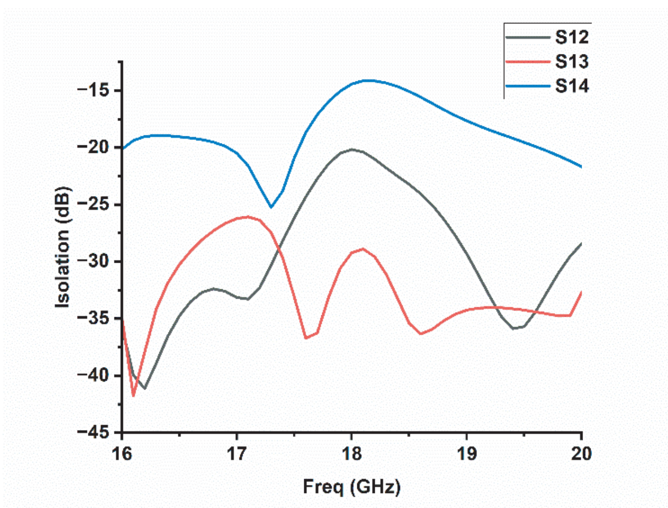

FIGURE 5. Isolation of MIMO antenna (simulated).

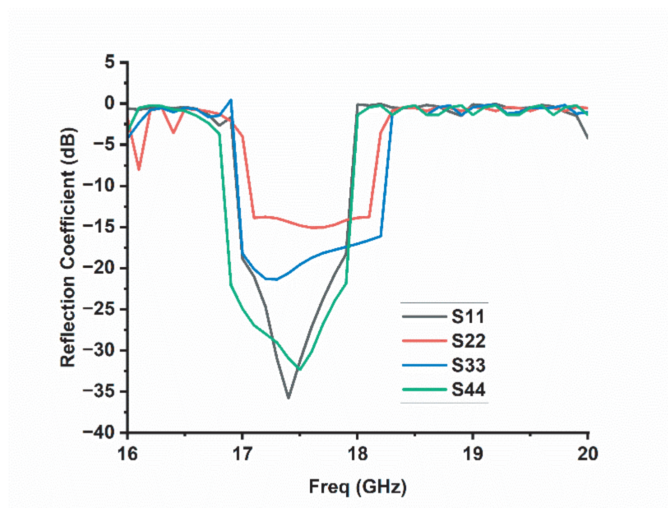

FIGURE 6. Reflection Coefficient of MIMO antenna (simulated).

TABLE 1. Dimensions.

S. No	Dimensions	Value (in mm)
1.	l_{eff}	36
2.	W_{eff}	36
3.	h	1.57
4.	d	0.5
5.	p	2
6.	l_1	11
7.	l_2	5

For achieving a complete planar configuration, for feeding the antenna, a 50 Ω microstrip line is used. The 4 elements of the MIMO antenna show the isolation of 20 dB, as shown in Fig. 5.

To maintain the simplicity and integrity of the proposed MIMO antenna, the four different elements of antenna are placed on the upper plane, and all elements share common ground plane. The reflection coefficient of each element of MIMO is shown in Fig. 6. The interpretation which can be achieved from Fig. 6 is that the complete operating range of the proposed antenna is **16.9 dB to 17.9 dB** which lies in the **Ku** band for satellite applications. The bandwidth of each element of the MIMO is 1 GHz (approximately) which help in increasing its channel capacity.

4. MIMO PROPERTIES

The performance of the proposed MIMO antenna are justified in terms of various parameters:

1. Envelope correlation coefficient (ECC): — ECC tells us about the correlation between different elements of the MIMO

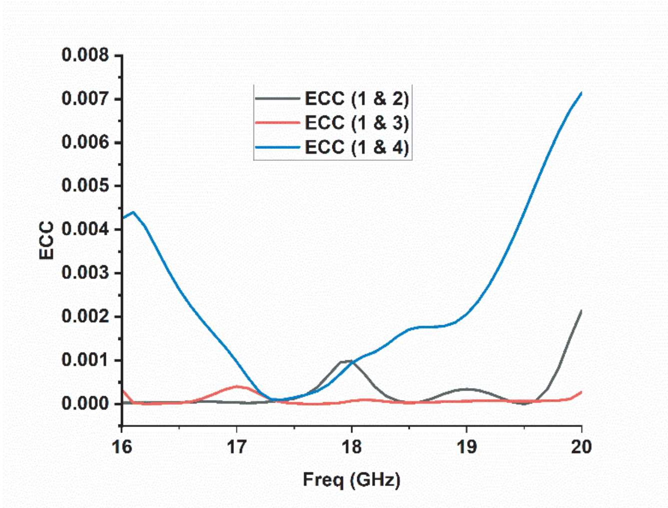

FIGURE 7. ECC of MIMO antenna.

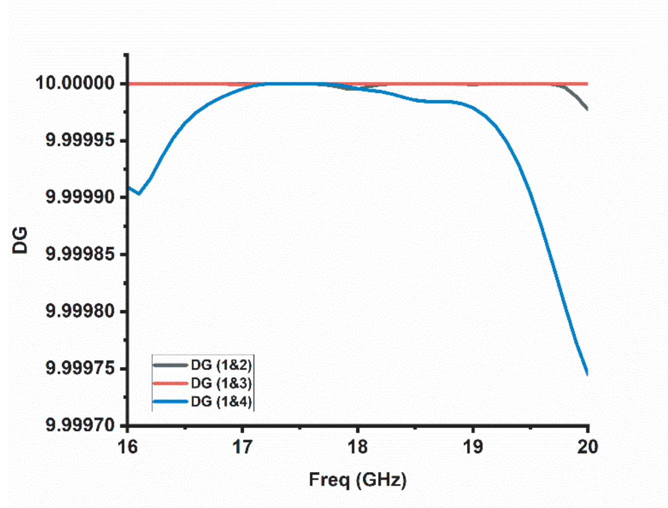

FIGURE 8. DG of MIMO antenna.

antenna and how different elements of MIMO antenna are operating independently. For good MIMO performance its value should be < 0.5. It can be derived from the formula shown below (2) [19, 20]

$$ECC = \frac{|S_{11} * S_{13} + S_{13}S_{33}|^2}{(1 - (|S_{11}|^2 + |S_{31}|^2)))(1 - (|S_{31}|^2 + |S_{13}|^2))} \tag{2}$$

Formula (2) is used when ECC has to be calculated between 1st and 3rd elements and when we want to calculate ECC between the 1st and 2nd elements, subscript 3 of formula has to be replaced with 2 and so on.

ECC which has been achieved in the proposed design has the maximum of 0.0010 between the 1st and 2nd elements, 0.00040 between the 1st and 3rd elements, 0.0013 between the 1st and 4th elements in the operating range of the MIMO. For MIMO antenna, ECC tells us how much the different elemental antennas of MIMO are working independently. Its value should be as low as possible, and the most accepted value for performance of MIMO is below 0.5. So, we can interpret that the proposed MIMO is in good agreement as its value is below 0.5 in all cases as shown in Fig. 7.

2. Diversity Gain (DG): — Diversity Gain is also one of the important performance characteristics of the MIMO antenna which tells us the signal to interference ratio due to the application of diversity scheme or rise in gain of MIMO antenna due to multiple elements. Its ideal value is approximately 10 when being expressed in ratio. It can be derived from the formula shown below (3) [19, 20]

$$DG = 10\sqrt{1 - 1 - |0.99ECC|^2} \tag{3}$$

The DG i.e., the diversity gain, which shows the increase in signal to interference ratio due to any diversity scheme is also above 10 in all the elements of proposed MIMO as shown in Fig. 8.

3. Total active reflection Coefficient (TARC): — Return loss of the antenna is the most important parameter that signifies its performance. TARC defines the return loss of MIMO antenna, and mathematically it is the ratio of the square root of total reflected power by the square root of total incident power.

It is given by formula (4) [19, 20]

$$TARC = \frac{\sqrt{(|S_{ii} + S_{ij}e^{j\theta}|^2 + |S_{ji} + S_{jj}e^{j\theta}|^2)}}{\sqrt{2}} \tag{4}$$

where S_{ii} and S_{jj} are the reflection coefficient between elements of MIMO whose TARC has to be calculated. Similarly, S_{ij} and S_{ji} are transmission coefficient. The desirable value of TARC is < 0 dB.

As shown in Fig. 9, the TARC value between different elements of the proposed MIMO antenna is below 2 dB which is in good agreement with the desirable standard value which is below 0 dB.

4. Channel Capacity Loss (CCL): — CCL is another important performance parameter of MIMO antenna which tells us about the channel capacity loss, and it is calculated using formula (5) [19, 20] given below:

$$CL = -\log_2 det(\psi^R) \tag{5}$$

where ψ^R is the correlation matrix of receiving antenna, and it is expressed by formula (6) given below:

$$\psi^R = \begin{pmatrix} \psi_{ii} & \psi_{ij} \\ \psi_{ji} & \psi_{jj} \end{pmatrix} \tag{6}$$

where ψ_{ii}, ψ_{ij}, ψ_{ji} and ψ_{jj} are shown by Equations (7), (8), (9), and (10) respectively.

$$\psi_{ii} = 1 - (|S_{ii}|^2 + |S_{ij}|^2) \tag{7}$$
$$\psi_{ij} = -(S_{ii} * S_{ij} + S_{ji} * S_{ii}) \tag{8}$$
$$\psi_{ji} = -(S_{jj} * S_{ji} + S_{ij} * S_{jj}) \tag{9}$$
$$\psi_{jj} = 1 - (|S_{jj}|^2 + |S_{ji}|^2) \tag{10}$$

CCL less than 0.4 bits/sec/Hz is an acceptable value in the case of MIMO antenna.

The CCL value between different elements of proposed antenna in the operating frequency range is between

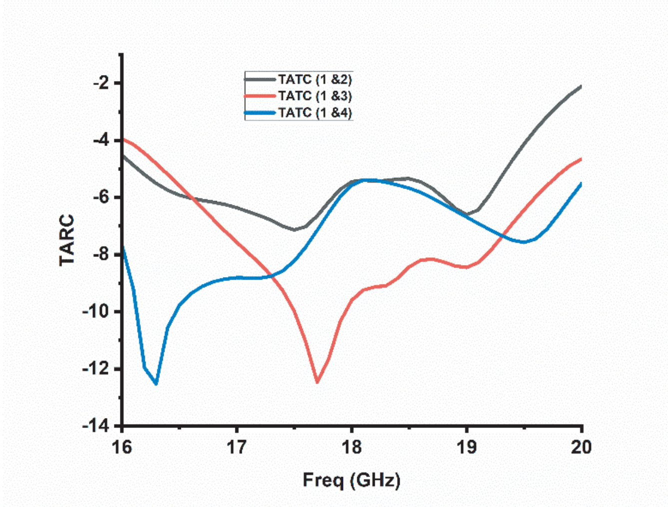

FIGURE 9. TARC of MIMO antenna.

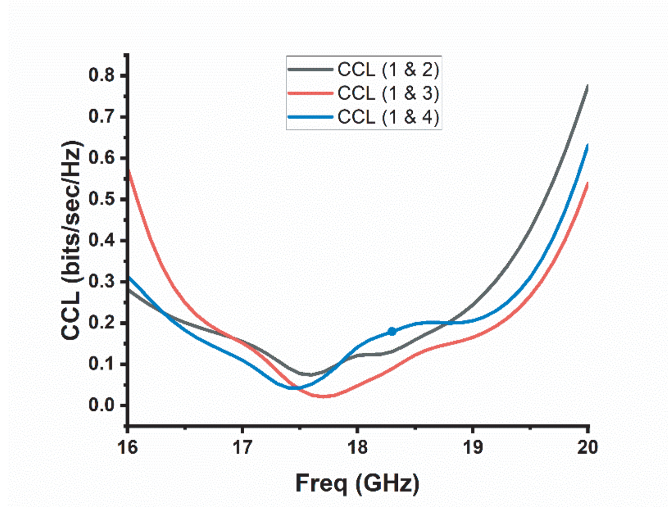

FIGURE 10. CCL of MIMO antenna.

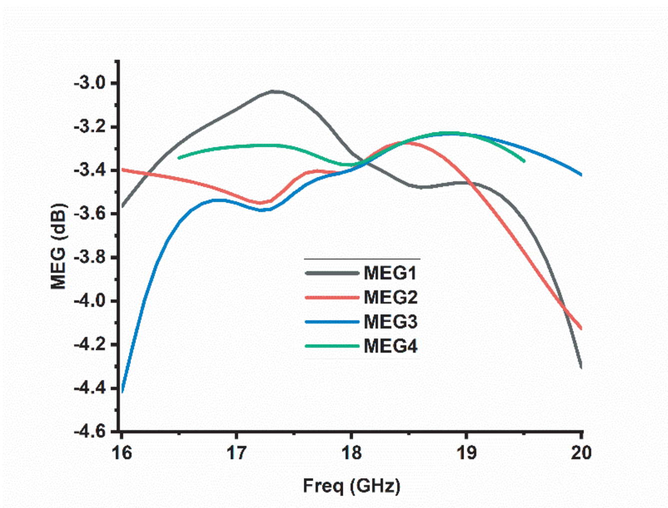

FIGURE 11. MEG of MIMO antenna.

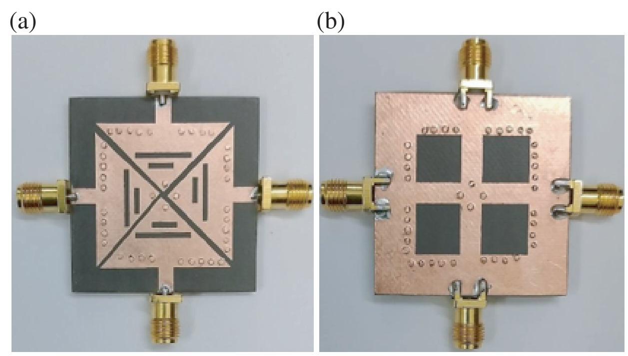

FIGURE 12. Fabricated antenna. (a) Top view. (b) Bottom View.

0.2 bits/sec/Hz and 0.0 bits/sec/Hz which agrees with the acceptable value of MIMO antenna as shown in Fig. 10.

5. Mean Effective Gain (MEG): — MEG is another performance parameter of MIMO antenna which tells the ratio of the average power absorbed to the incident power of the antenna and given by the formula (11) [19, 20].

$$MEG_i = 0.5\left(1 - \Sigma_i^N |S_{ij}|^2\right) \tag{11}$$

where i indicates the antenna which is active at particular moment whereas N indicates the total count of antenna element in designed MIMO.

The MEG value of respective antenna element of the MIMO can be calculated by Equations (12), (13), (14), and (15) [19, 20].

$$MEG_1 = 0.5(1 - |S_{11}|^2 - |S_{12}|^2 - |S_{13}|^2 - |S_{14}|^2) \tag{12}$$

$$MEG_2 = 0.5(1 - |S_{21}|^2 - |S_{22}|^2 - |S_{23}|^2 - |S_{24}|^2) \tag{13}$$

$$MEG_3 = 0.5(1 - |S_{31}|^2 - |S_{32}|^2 - |S_{33}|^2 - |S_{34}|^2) \tag{14}$$

$$MEG_4 = 0.5(1 - |S_{41}|^2 - |S_{42}|^2 - |S_{43}|^2 - |S_{44}|^2) \tag{15}$$

The desirable value of MEG for MIMO antenna should be between -3 dB and -12 dB. The obtained value of MEG for different antenna elements of proposed MIMO is shown in Fig. 11 which clearly shows that the proposed MIMO antenna satisfies the criterion.

5. RESULTS --- VALIDATION AND DISCUSSION

The antenna is designed and simulated using HFSS, Version 2019. The dimensional statistics are already given in Fig. 4(a) and Table 1. The boundary as per the lowest operating frequency of 16.9 GHz is $\lambda/4$, i.e., 4.44 mm, which is rounded to 4.50 mm on each side of the antenna to form a three-dimension radiating boundary. The iterations are calculated at 0.01 mm with surface normal deviation of 22.5 degrees. The mesh analysis method is classic mesh. The antenna is fabricated using printed circuit board (PCB) prototyping milling machine.

The proposed 4×4 antenna is fabricated on Rogers-5880, having relative permittivity 2.33, permeability 1, dielectric loss tangent 0.0012, thickness 1.57 mm, and dielectric constant of

(a) (b)

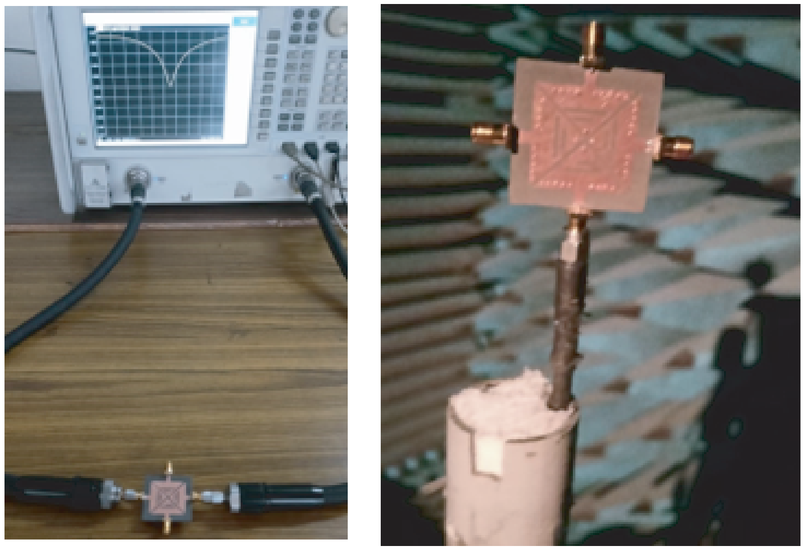

FIGURE 13. Fabricated antenna under testing. (a) VNA. (b) Anechoic chamber.

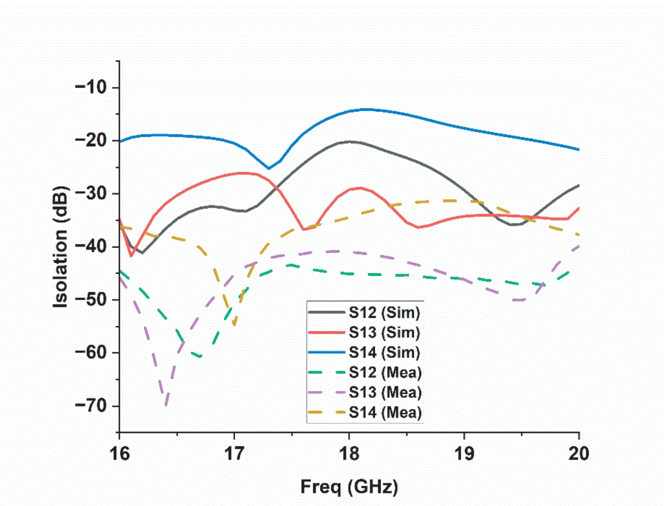

FIGURE 14. Comparison of Isolation coefficient of Simulated and Fabricated antenna.

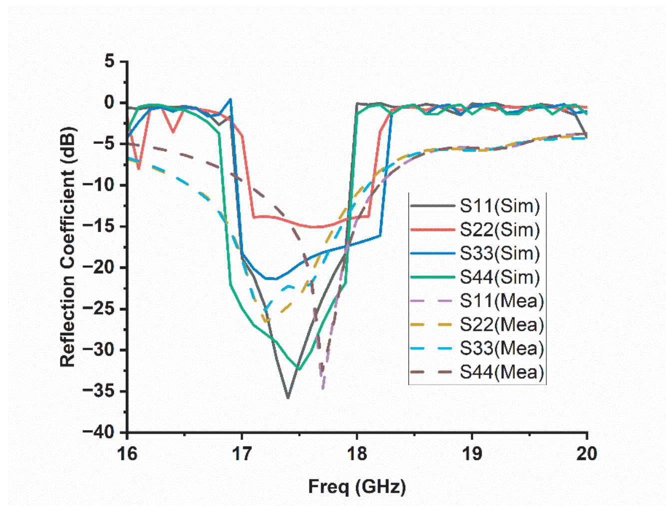

FIGURE 15. Comparison of Reflection Coefficient of Simulated and Fabricated antenna.

2.2 as shown in Fig. 12. The lower value of dielectric constant increases the antenna performance. Substrate material with both low dielectric loss tangent and low permittivity is required to improve the dielectric loss.

After fabrication, the proposed antenna is tested for its practical realization using VNA and an anechoic chamber as shown in Fig. 13. The simulated S-parameter results are shown in Figs. 5 and 6. Comparison of simulated results with the measured results of fabricated one is shown in Figs. 14 and 15.

On analysing Fig. 14 which shows the isolation between different elements of antennas of fabricated and simulated ones, it is clearly interpreted that a better isolation is achieved in the case of fabricated one with the isolation parameter below 40 dB within operating range which is 10–20 dB lower than the simulated one. Therefore, it can be easily said that a MIMO antenna which is designed/fabricated is good for practical use. The comparison between reflection coefficients of simulated and fabricated ones, as shown in Fig. 15, can be interpreted that they are approximately similar in the two cases with only a reduction of 20% bandwidth in fabricated one as compared to simulated one.

The measurements are conducted in an anechoic chamber of dimensions 8 feet of length, 5 feet of breadth, and 6 feet of height. Two horn antennas are taken with the range of 0.8 GHz to 18 GHz with voltage standing wave ratio (VSWR) less than 1.1 for this range and 18 GHz to 40 GHz with VSWR less than 1.0 for this range. For gain and radiation pattern measurements, the antenna is placed on an Automated Positioner System (Receiver) where the transmitter is kept fixed. All the parameters were measured using Vector Network Analyzer (Model-S820E) of measurement range 1 MHz to 30 GHz. The VNA was cal-

TABLE 2. Comparison of MIMO antenna with previous existing work.

Reference	Size (mm^3)	No. of antenna element	Frequency of operation (GHz)	Gain (dB)	Isolation (dB)	DG	ECC	CCL (bit/s/Hz)
[15]	$24 \times 24 \times 0.835$	4	24.8–44.45	8.6	> -20	9.96	< 0.007	-
[16]	$35 \times 30 \times 1.6$	4	8.5–12.5 GHz	6 dB	> -22	> 9.96	< 0.005	< 0.4
[17]	$20 \times 40 \times 1.6$	4	28 GHz	7.8	-29.34	9.96	0.05	-
[18]	$24 \times 24 \times 0.254$	4	25–39	7.1	-26	-	< 0.05	-
[19]	$30 \times 35 \times 0.76$		28 GHz	8.3	-10	9.96	0.05	0.4
Proposed work	$36 \times 36 \times 1.57$	4	16.9–17.9	5.73	-35	10	0.00040	0.2–0.00

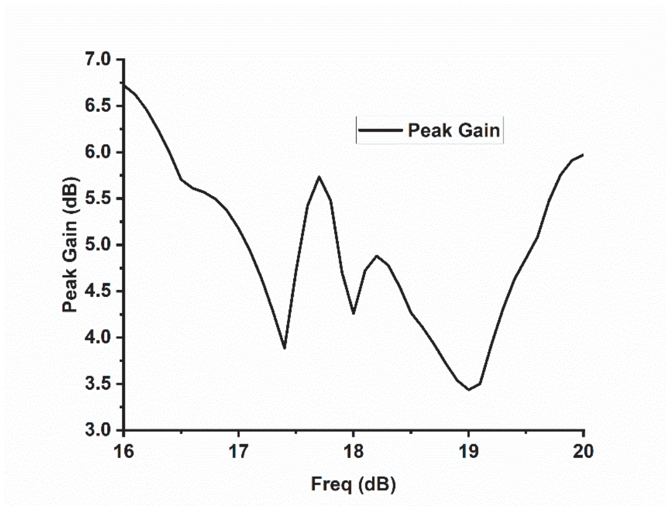

FIGURE 16. Peak Gain of MIMO antenna.

ibrated before all the measurements to nullify the impedance added by the coaxial cable.

The maximum peak gain of MIMO antenna obtained in far-field region in dB is 5.73 dB which is again a good value. Table 2 tabulates the recently published papers compared to the proposed paper and shows substantial improvement in isolation and other MIMO properties.

6. CONCLUSION

In this paper, a detailed analysis of a QMSIW based MIMO antenna has been presented with step by step evolution and improvement. It is presented that with reducing the structure from full mode to quarter mode the operating frequency range does not get disturbed. Then using quarter mode SIW for designing a 4×4 MIMO antenna, the antenna property gets improved which is shown in Figs. 14–16. Also good MIMO antenna properties are achieved which are shown in Figs. 7–11.

REFERENCES

[1] Thummaluru, S. R., R. Kumar, and R. K. Chaudhary, "Isolation enhancement and radar cross section reduction of MIMO antenna with frequency selective surface," *IEEE Transactions on Antennas and Propagation*, Vol. 66, No. 3, 1595–1600, 2018.

[2] Rosaline, I., A. Kumar, P. Upadhyay, and A. H. Murshed, "Four element MIMO antenna systems with decoupling lines for high-speed 5G wireless data communication," *International Journal of Antennas and Propagation*, Vol. 2022, No. 3, 1–13, 2022.

[3] Alazemi, A. J. and A. Iqbal, "A high data rate implantable MIMO antenna for deep implanted biomedical devices," *IEEE Transactions on Antennas and Propagation*, Vol. 70, No. 2, 998–1007, 2022.

[4] Boukarkar, A., X. Q. Lin, Y. Jiang, L. Y. Nie, P. Mei, and Y. Q. Yu, "A miniaturized extremely close-spaced four-element dual-band MIMO antenna system with polarization and pattern diversity," *IEEE Antennas and Wireless Propagation Letters*, Vol. 17, No. 1, 134–137, 2018.

[5] Sharma, N., A. Kumar, A. De, and R. K. Jain, "Isolation enhancement using CSRR Slot in the ground for compact two-element textile MIMO antenna," *ACES Journal*, Vol. 37, No. 5, 535–545, 2022.

[6] Zhai, G., Z. N. Chen, and X. Qing, "Enhanced isolation of a closely spaced four-element MIMO antenna system using metamaterial mushroom," *IEEE Transactions on Antennas and Propagation*, Vol. 63, No. 8, 3362–3370, 2015.

[7] Kumar, A., D. Saxena, P. Jha, and N. Sharma, "Compact two-port antenna with high isolation based on the defected ground for THz communication," *Results in Optics*, Vol. 13, No. 6, 100522, 2023.

[8] Deng, J., J. Li, L. Zhao, and L. Guo, "A dual-band inverted-F MIMO antenna with enhanced isolation for WLAN appli-

cations," *IEEE Antennas and Wireless Propagation Letters*, Vol. 16, 2270–2273, 2017.

[9] Cheong, P., K.-F. Chang, W.-W. Choi, and K.-W. Tam, "A highly integrated antenna-triplexer with simultaneous three-port isolations based on multi-mode excitation," *IEEE Transactions on Antennas and Propagation*, Vol. 63, No. 1, 363–368, Jan. 2015.

[10] Dhwaj, K., X. Li, L. J. Jiang, and T. Itoh, "Low-profile diplexing filter/antenna based on common radiating cavity with quasi-elliptic response," *IEEE Antennas and Wireless Propagation Letters*, Vol. 17, No. 10, 1783–1787, 2018.

[11] Kumar, A., D. Chaturvedi, and S. I. Rosaline, "Design of antenna-multiplexer for seamless on-body internet of medical things (IoMT) connectivity," *IEEE Transactions on Circuits and Systems II: Express Briefs*, Vol. 69, No. 8, 3395–3399, 2022.

[12] Kumar, A. and A. A. Althuwayb, "SIW resonator-based duplex filtenna," *IEEE Antennas and Wireless Propagation Letters*, Vol. 20, No. 12, 2544–2548, 2021.

[13] Kumari, R. and S. Srivastava, "Gain enhancement at selective frequency of HMSIW based leaky wave antenna," *International Journal of Microwave & Optical Technology*, Vol. 18, No. 3, 256, 2023.

[14] Kumari, R. and S. Srivastava, "Leaky wave antenna in Quarter mode SIW filter," in *2022 International Conference for Advancement in Technology (ICONAT)*, 1–5, IEEE, 2022.

[15] Ahmad, U., S. Ullah, U. Rafique, D.-Y. Choi, R. Ullah, B. Kamal, and A. Ahmad, "MIMO antenna system with pattern diversity for sub-6 GHz mobile phone applications," *IEEE Access*, Vol. 9, 149 240–149 249, 2021.

[16] Ibrahim, A. A., H. Zahra, S. M. Abbas, M. I. Ahmed, G. Varshney, S. Mukhopadhyay, and A. Mahmoud, "Compact four-port circularly polarized MIMO X-band DRA," *Sensors*, Vol. 22, No. 12, 4461, 2022.

[17] Murthy, N., "Improved isolation metamaterial inspired mm-Wave MIMO dielectric resonator antenna for 5G application," *Progress In Electromagnetics Research C*, Vol. 100, 247–261, 2020.

[18] Khan, M. A., A. G. A. Harbi, S. H. Kiani, A. N. Nordin, M. E. Munir, S. I. Saeed, J. Iqbal, E. M. Ali, M. Alibakhshikenari, and M. Dalarsson, "MmWave Four-element MIMO antenna for future 5G systems," *Applied Sciences*, Vol. 12, No. 9, 4280, 2022.

[19] Hussain, M., W. A. Awan, E. M. Ali, M. S. Alzaidi, M. Alsharef, D. H. Elkamchouchi, A. Alzahrani, and M. F. A. Sree, "Isolation improvement of parasitic element-loaded dual-band MIMO antenna for mm-Wave applications," *Micromachines*, Vol. 13, No. 11, 1918, 2022.

[20] Jetti, C. R., T. Addepalli, S. R. Devireddy, G. K. Tanimki, A. J. A. Al-Gburi, Z. Zakaria, and P. Sunitha, "Design and analysis of modified U-shaped four element MIMO antenna for dual-band 5G millimeter wave applications," *Micromachines*, Vol. 14, No. 8, 1545, 2023.